

L2PF - Learning to Prune Faster

Manoj-Rohit Vemparala^{*1}, Nael Fafous^{*2}, Alexander Frickenstein^{*1},
 Mhd Ali Moraly^{*1}, Aquib Jamal¹, Lukas Frickenstein¹,
 Christian Unger¹ Naveen-Shankar Nagaraja¹ Walter Stechele²
^{*} indicates equal contributions

¹ BMW Autonomous Driving

² Technical University of Munich

¹firstname.lastname@bmw.de, ²firstname.lastname@tum.de

Abstract. Various applications in the field of autonomous driving are based on convolutional neural networks (CNNs), especially for processing camera data. The optimization of such CNNs is a major challenge in continuous development. Newly learned features must be brought into vehicles as quickly as possible, and as such, it is not feasible to spend redundant GPU hours during compression. In this context, we present Learning to Prune Faster which details a multi-task, try-and-learn method, discretely learning redundant filters of the CNN and a continuous action of how long the layers have to be fine-tuned. This allows us to significantly speed up the convergence process of learning how to find an embedded-friendly filter-wise pruned CNN. For ResNet20, we have achieved a compression ratio of $3.84\times$ with minimal accuracy degradation. Compared to the state-of-the-art pruning method, we reduced the GPU hours by $1.71\times$.

1 Introduction

With the advent of scalable training hardware and frameworks, the trend towards training larger deep neural networks (DNNs) or ensembles of networks has become more prevalent than ever [8]. As a result, compression of DNNs has become an increasingly popular field of research in recent years. This is particularly the case for convolutional neural networks (CNNs), which have become the state-of-the-art solution for most computer vision problems, and often find applications in embedded scenarios, necessitating a reduction in their storage requirements and computational costs for inference. In the field of autonomous driving [4], embedded hardware [2, 18] is highly constrained and short development cycles are key for being first to market.

Many standard techniques exist in literature to reduce the number of network parameters and the complexity of the computations involved in CNNs [8, 11]. Due to their inherent complexity and redundancy, CNNs can sustain many forms of structural and algorithmic approximation while still delivering adequate functional accuracy w.r.t. the given task, e.g. image classification. With the help of

fine-tuning iterations, CNNs can recover the lost accuracy after a compression method has been applied, with negligible degradation.

Network compression can be viewed as a standard optimization problem. The search space composes of the possible combinations to compress neurons, kernels or layers. Exploring this design space is a difficult task when considering its size and the computational overhead required to sufficiently evaluate each potential configuration in it. Referring back to the healing effect of network fine-tuning after pruning, efficiently traversing this search space necessitates a fair balance between the number of epochs the fine-tuning is done for and the computational overhead required by those fine-tuning epochs. This ultimately leads to shorter product and time-to-market cycles and facilitates continuous development.

As with many other optimization problems, existing literature covers various forms of design space exploration w.r.t. pruning [9, 12, 20]. Automated pruning was an inevitable step in the evolution of this compression technique due to its complex nature. Automated pruning makes tools usable for researchers and product developers with little to no background in CNN optimization.

In this work, we build upon a learning-based pruning approach [12] to tackle the challenge of choosing the optimal number of fine-tuning epochs³ for a potential pruning solution. The decisions of our RL-based pruning agent are based not only on the features embedded in the CNNs kernels, but also on the fine-tuning potential of the individual layers. This results in feature-conscious decisions and reduced overall time required by the pruning technique. The contributions of this paper can be summarized as follows:

- A multi-task learning approach involving a reinforcement learning agent, which learns a layer’s features and adequate fine-tuning time concurrently.
- Formalizing the design space exploration problem w.r.t. pruning effectiveness and time-effort.
- A study on the sequence of layer-wise pruning of a convolutional neural network.

2 Related Work

In the following sections, we classify works which use pruning techniques into heuristic-based, in-train and learning-based strategies.

Heuristic-based Pruning: Heuristic-based compression techniques consider static or pseudo-static rules that define the compression strategy, when pruning an underlying CNN. The pruning method proposed by [6] utilizes the magnitude of weights, where values below a threshold identify expendable connections. Such pruning of individual weights, as presented in [6], leads to inefficient memory accesses, rendering irregular pruning techniques impractical for most general purpose computing platforms. Regularity in pruning is a key factor in

³ An epoch describes a complete cycle of a data set, *i.e.* training data set.

accelerator-aware optimization. Frickenstein et al. [5] identifies redundant kernels in the weight matrix based on magnitude based heuristic. He et al. [10] prune redundant filters based on the geometric median heuristic of the filters. In [11], He et al. introduce an iterative two-step algorithm to effectively prune layers in a given CNN. First, redundant feature maps are selected by LASSO regression followed by minimizing the output errors of the remaining feature maps by solving least squared minimization.

In-train Pruning: Integrating the pruning process into the training phase of CNNs is characterized as in-train pruning. The auto-encoder-based low-rank filter-sharing technique (ALF) proposed by Frickenstein et al. [3] utilizes sparse auto-encoders that extract the most salient features of convolutional layers, pruning redundant filters. Zhang et al. [22] propose ADAM-ADMM, a unified, systematic framework of structured weight pruning of DNNs, that can be employed to induce different types of structured sparsity based on ADMM.

Learning-based Pruning: Defining the pruning process as an optimization problem and exposing it to an RL-agent has been done in a variety of works [9, 12]. He et al. [9] demonstrate a channel pruning framework leveraging a Deep Deterministic Policy Gradient (DDPG) agent. Their framework first learns the sparsity ratio to prune a layer, while actual channel selection is performed using ℓ_1 criteria. The appealing higher compression ratio, better preservation of accuracy as well as faster, coarse and learnable exploration of the design space with few GPU hours, highlight the strong points of the AMC framework. However, this leaves room for improvement in search-awareness, as AMC is unaware of the exact features it is pruning. Huang et al. [12] demonstrated a 'try-and-learn' RL-based filter-pruning method to learn both sparsity ratio and the exact position of redundant filters, but it leaves out the number of fine-tuning epochs as a hyper-parameter. Here, the optimal value can change, depending on the model's architecture and the data set at hand. We extend the work of Huang et al. [12] incorporating GPU hour awareness by proposing an iterative method with a learned minimum number of iterations for fine-tuning, hyper-parameter free method.

3 Method

In this chapter, we propose a multi-task learning approach, namely *Learning to Prune Faster* (L2PF) involving a RL-agent, which learns a layer's features and adequate fine-tuning time concurrently. In this regard, the pruning problem in the context of a RL framework is formulated in Sec. 3.1. The environment and state space is defined in Sec. 3.2. We discuss the discrete and continuous action spaces in Sec. 3.3, and the reward formulation in Sec. 3.4. Lastly, the agent's objective function is formulated in Sec. 3.5.

3.1 Problem Formulation

The structured filter-pruning task within an RL framework can be expressed as a 'try-and-learn' problem, similar to the work from Huang et al. [12]. We

aim to find the best combination of filters that achieve the highest compression ratio (CR) while incurring a minimum loss of accuracy (Acc) and requiring a minimum number of fine-tuning epochs during the exploration episodes. Fig. 1 demonstrates the interplay between the proposed pruning agent and CNN environment. The proposed method is able to learn three aspects: First, the minimum number of epochs required to explore each pruning strategy. Second, the degree of sparsity of each layer in the model. Third, the exact position of the least important filters to be pruned.

Formally, let B be a fully-trained model with L layers and the input of the ℓ^{th} convolutional layer has a shape $[c^\ell \times w^\ell \times h^\ell]$, where c^ℓ , h^ℓ and w^ℓ represents number of input channels, height and width. The ℓ^{th} layer is convolved with the weight tensor \mathbf{W}^ℓ , *i.e.* 2D convolutional layer’s trainable parameters, with shape $[N^\ell \times c^\ell \times k^\ell \times k^\ell]$, where k^ℓ represents the kernel size and N^ℓ is number of filters. After pruning n^ℓ filters, the weight tensor is of shape $[(N^\ell - n^\ell) \times c^\ell \times k^\ell \times k^\ell]$. To enable a direct comparison with the work of He et al. [9], the layer compression ratio is defined as $\frac{c^\ell - n^{\ell-1}}{c^\ell}$. Additionally, we define model compression ratio to be the total number of weights divided by the number of non-zero weights.

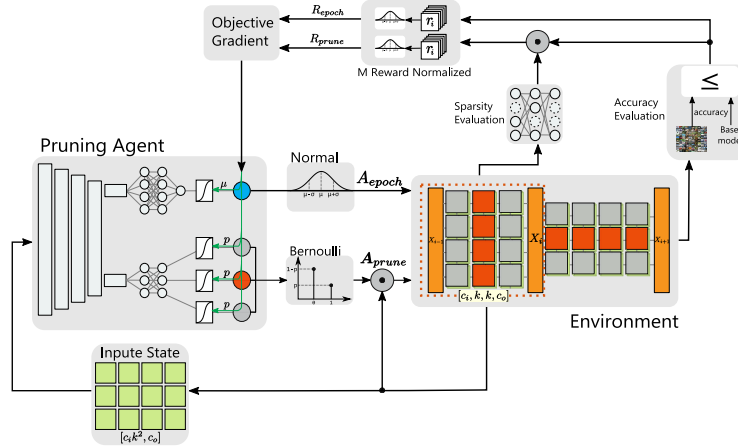


Fig. 1: Agent receives rewards and weights as input state, whereas environment receives both prune and epoch actions. In each prune episode, $M=5$ Monte-Carlo set of actions are sampled (\mathbf{A}_{prune} and $A_{retrain}$). The corresponding M rewards (R_{prune} and $R_{retrain}$) are normalized to zero mean and unit variance [12].

3.2 Environment

The environment is the pre-trained CNN model B to be pruned. The **state space** is the fully trained weight tensor \mathbf{W}^ℓ of the layer to be pruned, which is used as an input for the agent, similar to Huang et al. [12]. For each layer (or residual block), a new agent is trained from scratch. The environment receives

two actions from the agent: pruning action $\mathbf{A}_{\text{prune}}$ and fine-tuning epoch action A_{retrain} . Subsequently, it generates a reward $R = R_{\text{prune}} + R_{\text{retrain}}$. For each filter there is a binary mask $\mathbf{m}_i^\ell \in \{0, 1\}^{c^\ell \times k^\ell \times k^\ell}$. Pruning the i^{th} filter \mathbf{W}_i^ℓ in layer ℓ is performed by element-wise multiplication between the filter \mathbf{W}_i^ℓ and its corresponding mask \mathbf{m}_i^ℓ . When pruning \mathbf{W}_i^ℓ , the i^{th} kernel of all filters in the $(\ell + 1)^{\text{th}}$ layer are also pruned. At each pruning step, masks are updated according to $\mathbf{A}_{\text{prune}}$ and the environment is fine-tuned for a few epochs e_{retrain} .

3.3 Distinct Action Space for Pruning and Epoch-Learning

The action space of the proposed RL-framework is split into two distinct spaces to satisfy the discrete and continuous requirements of actions for pruning and epoch learning respectively.

Discrete Pruning Action Space: The discrete pruning action space is the combination of all possible prune actions $\mathbf{A}_{\text{prune}}$. It is clear that action space dimension grows exponentially as $\mathcal{O}(2^N)$, where N is the number of filters in a layer. Discrete actions are sampled from N independent stochastic Bernoulli units [19]. Each unit has one learnable parameter p that represents the probability of keeping the filter.

Continuous Epoch-Learning Action Space: The continuous epoch-learning is used to determine the number of fine-tuning epochs e_{retrain} . Like the discrete action, the continuous action A_{retrain} must also be sampled from some distribution. Practically, e_{retrain} takes values within a bounded range $\in \mathbb{Q}^+$. A continuous action A_{retrain} is sampled from a Normal distribution which has two learnable parameters μ and σ . Since e_{retrain} is bounded while Normal distribution has unbounded support, it must be truncated. Truncating a Normal distribution might cause the estimated policy to get biased into the direction of the truncation boundary where the reward peaks (boundary effect) [1]. To circumvent the boundary effect, we employ the approach from Chou et al. [1]. The sampled action A_{retrain} is sent to the environment with no alteration. To calculate e_{retrain} , the action value is truncated within $[0, 1]$. However, for gradient calculations, non-truncated action values are used.

3.4 Multi-objective Reward Function

The quality of agent action is conveyed back to the agent by the reward signal, R_{prune} and R_{retrain} for $\mathbf{A}_{\text{prune}}$ and A_{retrain} respectively.

Prune Reward: The prune reward R_{prune} is a measure for sparsity level and model accuracy acc_{pruned} . It promotes actions that remove filters with minimum accuracy loss of the pruned model w.r.t. the validation set. Following the work of Huang et al. [12], we define the prune reward as a product of two terms, *i.e.* acc_{term} and eff_{term} , as stated in Eq. 1.

$$R_{\text{prune}}(\mathbf{A}_{\text{prune}}^\ell, acc_{\text{pruned}}) = acc_{\text{term}} \cdot eff_{\text{term}} \quad (1)$$

Accuracy Term: Similar to Huang et al. [12], acc_{term} is defined in Eq. 2. The bound b is a hyper-parameter introduced in the reward function to allow control over the trade-off between model compression and tolerable accuracy drop. When the accuracy drop is greater than b , acc_{term} is negative, otherwise it lies in the range $[0, 1]$ respectively 0 and 100%.

$$acc_{\text{term}} = \frac{b - \max[0, acc_{\text{base}} - acc_{\text{pruned}}]}{b} \quad (2)$$

Efficiency Term: To prevent the agent from changing the model depth, the efficiency term eff_{term} proposed by Huang et al. [12] is extended as shown in Eq. 3. If the prune action is aggressive, the accuracy drop will be less than the bound b resulting in a negative reward. If layer sparsity ratio is low, eff_{term} will drive reward to zero.

$$eff_{\text{term}} = \begin{cases} \log \frac{N}{(N-n)} & \text{if } (N-n) \leq N \\ -1 & \text{if } (N-n) = 0 \end{cases} \quad (3)$$

Fine-tuning Epoch Reward: The fine-tuning epoch reward R_{retrain} is responsible for promoting a lower number of fine-tuning epochs. The reward is expressed in Eq. 4. An action is considered *good* when $|A_{\text{retrain}}|$ is low without causing an intolerable accuracy drop. If the environment incurs no accuracy loss then $R_{\text{retrain}} = 0$, when loss is incurred then it will be a negative value scaled by the absolute value of A_{retrain} .

$$R_{\text{retrain}}(A_{\text{retrain}}, acc_{\text{pruned}}) = |A_{\text{retrain}}| \times (acc_{\text{pruned}} - acc_{\text{base}}) \quad (4)$$

In each prune episode, M Monte-Carlo set of actions are sampled again resulting in M corresponding rewards R_{prune} and R_{retrain} . The reward values are normalized to zero mean and unit variance for both set of rewards [7, 14].

3.5 Agent Design

The agent is a non-linear stochastic functional approximator parameterized by θ . It is composed of four convolutional layers, two classifiers each with two feed-forward layers [12], and two types of stochastic output units, *i.e.* Bernoulli and Normal. The agent parameters are $\theta = \{\mathbf{w}, \mu, \mathbf{P}\}$, where parameters \mathbf{w} are the agent weights, μ is a learnable parameter to sample the fine-tuning action A_{retrain} , and \mathbf{P} is the set of probabilities for Bernoulli units. The agent outputs two actions: discrete action $\mathbf{A}_{\text{prune}}$ for pruning, and continuous action A_{retrain} for fine-tuning epochs.

The **pruning action** $\mathbf{A}_{\text{prune}}$ is a set $\{a_1^\ell, a_2^\ell, \dots, a_{N^\ell}^\ell\}$, where $a_i^\ell \in \{0, 1\}$ is equivalent to $\{\text{prune}, \text{keep}\}$ and N^ℓ is the number of filters in the ℓ^{th} layer [12]. Using this scheme, the agent is able to explore both sparsity ratio and to select the exact position of filters to prune.

The **fine-tuning action** A_{retrain} is a continuous action sampled from a normal distribution with two parameters - μ , σ . The mean μ is a learnable parameter, while σ is chosen to be non-learnable and set to be proportional to $|R_{\text{retrain}}|$ [17, 19]. The value of σ controls how far a sample can be from the mean. When reward signal R_{retrain} is low indicating bad actions, then σ takes higher value which allows the agent to explore actions further away from μ . Actions $A_{\text{retrain}} \notin [0, 1]$ are considered *bad* and give negative reward. The environment fine-tunes for the number of epochs given in Eq. 5, where β is an upper limit for e_{retrain} .

$$e_{\text{retrain}} = \min[\max[0, A_{\text{retrain}}], 1] \times \beta \quad (5)$$

We leverage the stochastic policy gradient (SPG) method to find an optimal policy π^* . SPG is guaranteed to converge at least to a local optimum without requiring the state space distribution [16]. Our objective function $J(\theta)$ is the expected sum of all rewards over one episode. The objective gradient w.r.t. the policy parameters is given in Eq. 6. Both terms in Eq. 6 can be solved approximately using the policy gradient theorem. Specifically, we implement a variant of SPG called REINFORCE [12, 19]. The agent parameters θ are updated with gradient ascent so that actions with higher rewards are more probable to be sampled [19].

$$\nabla_{\theta} J(\theta) = \nabla_{\theta} \mathbb{E}[r_{\text{prune}}] + \nabla_{\theta} \mathbb{E}[r_{\text{retrain}}] \quad (6)$$

The first term in Eq. 6 has the Bernoulli policy $\pi_B(\mathbf{A}_{\text{prune}}|\mathbf{W}^{\ell}, \mathbf{P}, \mathbf{w})$, while the second has the Normal policy $\pi_N(\mathbf{A}_{\text{retrain}}|\mathbf{W}^{\ell}, \mu, \mathbf{w})$, where \mathbf{W}^{ℓ} are weights for layer to prune. Finding a closed-form solution for the expectation is not feasible, so it is approximated using M samples of a Monte-Carlo gradient estimator with score function [14, 16]. The gradient of our objective function is given by Eq. 7.

$$\nabla_{\theta} J(\theta) \approx \sum_{j=1}^M \left[(R_{\text{prune}})_j \cdot \sum_{i=1}^n \frac{a_{ij} - p_{ij}}{p_{ij}(1 - p_{ij})} \cdot \frac{\partial p_{ij}}{\partial \mathbf{w}} + (R_{\text{retrain}})_j \cdot \frac{a_j - \mu_j}{\sigma_j^2} \cdot \frac{\partial \mu_j}{\partial \mathbf{w}} \right] \quad (7)$$

4 Experimental Results

Our experiments are conducted on the CIFAR-10 [13] data set. One-time random splitting of the 50k images into 45k training and 5k evaluation is performed. Agent reward is evaluated on 5k images. To ensure that our pruning method generalizes, the 10k images in the test data set are held separate and only used after the agent learns to prune a layer, to report actual model accuracy. No training or reward evaluation is performed using the test data set. As a baseline, ResNet-20 is trained from scratch as described in [8] until convergence with validation accuracy 92.0%, and test accuracy of 90.8%. After each pruning episode, the environment is retrained for a few epochs (8 w/o epochs learning) using mini-batch momentum SGD [15] with learning rate of 0.001, gamma 0.5, step size of 1900, batch size of 128, and l_2 regularization. After learning to prune a

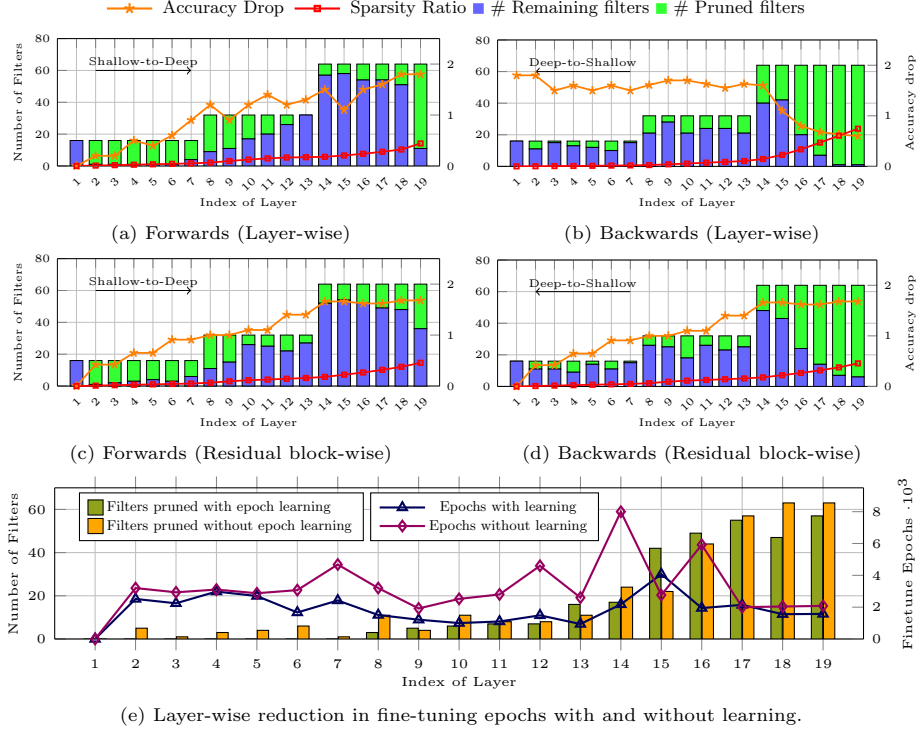


Fig. 2: Exploration of filter pruning order and epoch-learning effect.

layer, the model is fine-tuned for 150 epochs before moving to the next layer. The agent is also trained using mini-batch momentum SGD with fixed learning rate of 0.005 and batch size equal to the number of Monte-Carlo samples $M = 5$.

4.1 Design Space Exploration

Exploration of Efficient Pruning Order: We investigate four different strategies based on the pruning order and the agent’s capability to prune layers simultaneously (layerwise or blockwise). We exclude the first convolutional layer since pruning it offers insignificant compression benefits, while damaging the learning ability of the model. When pruning a full residual block, we preserve the element-wise summation by zero-padding the output channels of the second layer in a residual block to restore the original number of output channels, such that the order of pruned channels is preserved. Fig. 2 shows results of pruning ResNet-20 with loss bound b of 2%. In Fig. 2a, we perform layer-wise pruning following the forward pruning order (`conv2_1.1` \rightarrow `conv4_3.2`). The agent starts pruning initial layers aggressively and struggles to find redundant filters in the deep layers

Configuration	Pruning Order	Bound [%]	Learnable Epochs	Acc [%]	CR [\times]
ResNet-20 [8]	-	-	-	90.8	1.00
L2PF (Block-wise)	Forwards	2.0	\times	89.9 (-0.9)	1.84
L2PF (Layer-wise)	Forwards	2.0	\times	89.6 (-1.2)	1.79
L2PF (Block-wise)	Backwards	2.0	\times	89.5 (-1.3)	3.38
L2PF (Layer-wise)	Backwards	2.0	\times	89.9 (-0.9)	3.90
L2PF (Layer-wise)	Backwards	1.0	\times	90.2 (-0.6)	2.52
L2PF (Layer-wise)	Backwards	2.0	\times	89.9 (-0.9)	3.90
L2PF (Layer-wise)	Backwards	3.0	\times	89.2 (-1.0)	4.53
L2PF (Layer-wise)	Backwards	4.0	\times	88.5 (-2.3)	7.23
L2PF (Layer-wise)	Backwards	2.0	\times	89.9 (-0.9)	3.90
L2PF (Layer-wise)	Backwards	2.0	\checkmark	89.9 (-0.9)	3.84

Table 1: Evaluating various configurations for L2PF to analyze the influence of exploration granularity, pruning order, accuracy bound w.r.t. prediction accuracy and compression ratio.

(indicated by large blue bars). In Fig. 2b, we perform a similar layer wise pruning analysis for the backward pruning order (`conv2_1.1` \leftarrow `conv4_3.2`). From Tab. 1, we observe that the backward pruning order results in higher CR with lower accuracy degradation (0.9%). In Fig. 2c and 2d, we perform block wise pruning allowing the agent to prune the entire residual block simultaneously. Similar to layer-wise pruning, we prune the residual blocks both in forward and backward orders. Lower compression ratio is observed when compared to layer-wise pruning, see also Tab. 1. Thus, we prune layer-wise in backward order as it results in lower accuracy degradation and high CR for the subsequent experiments.

Effect of Accuracy Bound on Compression Ratio: In Tab. 1, we also evaluate the impact of the prediction accuracy and compression ratio by varying the agent’s loss bound b . As we increase b , we obtain higher CR with lower prediction accuracy after fine-tuning. We choose b as 2% to maintain a trade-off between accuracy degradation and CR.

Effect of Accuracy and Pruning Rate on Exploration Time: Previous experiments were conducted with fine-tuning epochs set manually to 8 at each exploration step. We allow the agent to decide the amount of fine-tuning time required to evaluate the pruning strategy based on the retrain epoch reward presented in Eq. 4. Fig. 2e shows a comparison of number of fine-tuning epochs required to decide the pruning strategy for each layer. Pruning with epochs learning achieves $1.71\times$ speedup in search time with a slight reduction in compression ratio, see Tab. 1.

4.2 Class Activation Maps

The discrete action space proposed by Huang et al. [12] and applied in L2PF (described in Sec.3.3) allows the integration of class activation mapping (CAM) [23] into the design process. CAM allows the visualization of regions of interest (RoI) in an input image to identify the corresponding prediction label. Regions with red color denote the part with higher interest for CNN model and blue denotes regions with less importance w.r.t. the target label. Tab. 2 shows three exemplary CAMs for the learned features of vanilla ResNet-20 and the influence of L2PF pruning (backwards) on the learned features and thus the RoIs. The progression of discriminative regions of classes can be compared across pruning steps.

In the first row, the vanilla ResNet-20 predicts the wrong class, *i.e.* *deer*. After pruning layer `conv3_3_2`, the RoI shifts towards the *trunk* of the *car* indicating the correct class. In the second row, the vanilla ResNet-20 predicts the *ship* class. The agent tries to retain the prediction across different stages of pruning with high confidence. In the third row, the vanilla ResNet-20 predicts the *truck* class. Accordingly, the pruned model at different stages also predict a *truck*. However, we can observe that the RoI becomes narrower indicating that the pruned model requires only few concentrated regions due to lower model capacity. We consider potential directions of our future work as follows: (1) Considering the CAM output as a state embedding instead of a weight matrix, making the pruning more feature-aware and interpretable. This would not possible with threshold


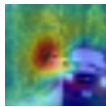
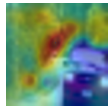



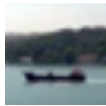
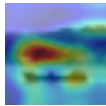
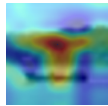
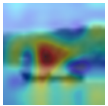
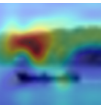
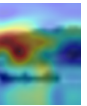
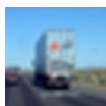
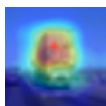
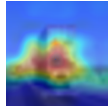
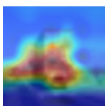
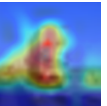

Input image	ResNet-20 unpruned	Learning to Prune Faster (Backwards)			
		<code>conv4_3_2</code> →	<code>conv3_3_2</code> →	<code>conv2_3_2</code> →	<code>conv2_1_2</code>
	 <i>deer</i> (0.53)				
raw		<i>car</i> (0.99) →	<i>car</i> (0.99) →	<i>car</i> (0.99) →	<i>car</i> (0.88)
	 <i>ship</i> (0.99)				
raw		<i>ship</i> (0.51) →	<i>ship</i> (0.98) →	<i>ship</i> (0.81) →	<i>ship</i> (0.99)
	 <i>truck</i> (0.99)				
raw		<i>truck</i> (0.98) →	<i>truck</i> (0.77) →	<i>truck</i> (0.62) →	<i>truck</i> (0.67)

Table 2: CAM visualization for three examples images from the validation dataset. Each column shows the CAM output after pruning, using backwards pruning order before model fine-tuning.

based approaches like AMC [9], (2) Understanding, the impact of feature-aware pruning on model robustness [21].

4.3 Comparison with the State-of-the-Art

In this section, we compare the proposed L2PF with other RL-based state-of-the-art filter pruning works proposed in literature. In Fig. 3, we compare our pruning configuration using layer-wise CR and final prediction accuracy with AMC [9], L2P [12], ALF [3]. We reimplemented L2P using forward pruning order with an accuracy bound $b=2\%$ to obtain pruning results for ResNet-20. Compared to L2P, we obtain 0.3% better prediction accuracy, $2.11\times$ higher CR and $1.71\times$ less fine-tune epochs. ALF and AMC do not require fine-tuning during the pruning process. Compared to AMC’s pruning implementation for Plain-20, we obtain $2.08\times$ higher CR with 0.3% lower prediction accuracy. Compared to ALF, we achieve 0.5% better accuracy with comparable CR.

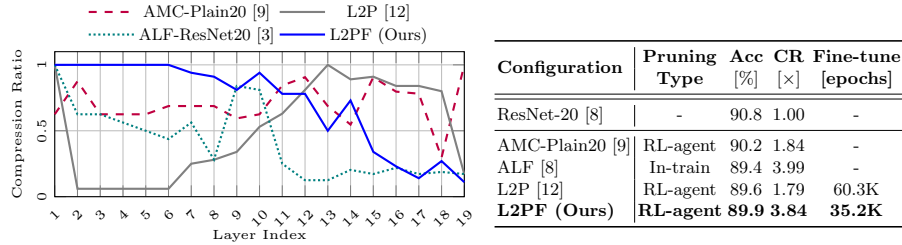


Fig. 3: Comparing L2PF pruning statistics on ResNet-20 with State-of-the-Art.

5 Conclusion

In this work, we demonstrated an RL-based filter-wise pruning method which is both feature and time-aware. Our multi-task approach achieved high compression ratios, while minimizing the required GPU-hours and the accuracy degradation. The analysis on the sequence of layer-wise pruning led to the conclusion that backward (deep-to-shallow) pruning can surpass the existing state-of-the-art compression ratios, with minimal degradation in task accuracy. Finally, we visually analyzed the effect of our pruning technique with the help of class activation maps to build a better understanding of our agent’s pruning decisions. GPU-hours for CNN compression can have many negative consequences on development cycles, profitability and fast exploration. The GPU-hour-aware approach presented can help mitigate this impediment and achieve a competitive advantage in active research fields such as autonomous driving.

References

1. Chou, P., Maturana, D., Scherer, S.: Improving stochastic policy gradients in continuous control with deep reinforcement learning using the beta distribution. In: ICML (2017)

2. Fafous, N., Vemparala, M.R., Frickenstein, A., Stechele, W.: OrthrusPE: Runtime Reconfigurable Processing Elements for Binary Neural Networks. In: DATE. Grenoble, France (2020)
3. Frickenstein, A., Vemparala, M.R., Fafous, N., Hauenschild, L., Nagaraja, N.S., Unger, C., Stechele, W.: ALF: Autoencoder-based low-rank filter-sharing for efficient convolutional neural networks. In: ICML (2020)
4. Frickenstein, A., Vemparala, M.R., Mayr, J., Nagaraja, N.S., Unger, C., Tombari, F., Stechele, W.: Binary DAD-Net: Binarized Driveable Area Detection Network for Autonomous Driving. In: ICRA (2020)
5. Frickenstein, A., Vemparala, M.R., Unger, C., Ayar, F., Stechele, W.: DSC: Dense-sparse convolution for vectorized inference of convolutional neural networks. In: CVPR-W (June 2019)
6. Han, S., Pool, J., Tran, J., Dally, W.: Learning both weights and connections for efficient neural network. In: NIPS (2015)
7. Hasselt, H.V., Guez, A., Hessel, M., Mnih, V., Silver, D.: Learning values across many orders of magnitude. In: NeurIPS (2016)
8. He, K., Zhang, X., Ren, S., Sun, J.: Deep residual learning for image recognition. In: CVPR (2016)
9. He, Y., Lin, J., Liu, Z., Wang, H., Li, L.J., Han, S.: AMC: AutoML for Model Compression and Acceleration on Mobile Devices. In: ECCV (2018)
10. He, Y., Liu, P., Wang, Z., Hu, Z., Yang, Y.: Filter pruning via geometric median for deep convolutional neural networks acceleration. In: Proceedings of the IEEE Conference on Computer Vision and Pattern Recognition (CVPR) (2019)
11. He, Y., Zhang, X., Sun, J.: Channel pruning for accelerating very deep neural networks. In: ICCV (2017)
12. Huang, Q., Zhou, S.K., You, S., Neumann, U.: Learning to Prune Filters in Convolutional Neural Networks. WACV (2018)
13. Krizhevsky, A., Nair, V., Hinton, G.: Cifar-10 (canadian institute for advanced research) <http://www.cs.toronto.edu/~kriz/cifar.html>
14. Mohamed, S., Rosca, M., Figurnov, M., Mnih, A.: Monte carlo gradient estimation in machine learning. CoRR **abs/1906.10652** (2019)
15. Ning, Q.: On the momentum term in gradient descent learning algorithms. Neural networks **12**(1), 145–151 (1999)
16. Sutton, R.S., A.-G.Barto: Reinforcement Learning: An Introduction. Adaptive Computation and Machine Learning series, MIT Press (2018)
17. Sutton, R., McAllester, D., Singh, S., Mansour, Y.: Policy gradient methods for reinforcement learning with function approximation. NIPS (1999)
18. Vemparala, M.R., Frickenstein, A., Stechele, W.: An efficient fpga accelerator design for optimized cnns using opencl. In: ARCS 2019 (2019)
19. Williams, R.J.: Simple statistical gradient-following algorithms for connectionist reinforcement learning. Machine learning **8**(3-4), 229–256 (1992)
20. Yang, T.J., Howard, A., Chen, B., Zhang, X., Go, A., Sandler, M., Sze, V., Adam, H.: Netadapt: Platform-aware neural network adaptation for mobile applications. In: ECCV (September 2018)
21. Ye, S., Xu, K., Liu, S., Cheng, H., Lambrechts, J.H., Zhang, H., Zhou, A., Ma, K., Wang, Y., Lin, X.: Adversarial robustness vs. model compression, or both? In: ICCV (October 2019)
22. Zhang, T., Zhang, K., Ye, S., Li, J., Tang, J., Wen, W., Lin, X., Fardad, M., Wang, Y.: ADAM-ADMM: A unified, systematic framework of structured weight pruning for dnns. CoRR **abs/1807.11091** (2018)

23. Zhou, B., Khosla, A., Lapedriza, A., Oliva, A., Torralba, A.: Learning deep features for discriminative localization (2015)